Desalination and Water Treatment
www.deswater.com

doi: 10.1080/19443994.2015.1061953

57 (2016) 13561–13572
June

Taylor & Francis
Taylor & Francis Group

Application of modified clays as an adsorbent for the removal of Basic Red 46 and Reactive Yellow 181 from aqueous solution

Feriel Bouatay*, Sonia Dridi-Dhaouadi, Neila Drira, Mohamed Farouk Mhenni

Faculty of Sciences, Department of Chemistry, Research Unit of Applied Chemistry & Environment, University of Monastir, Monastir 5019, Tunisia, Tel. +216 22 853 652; Fax: +216 73 500 278; emails: bouatay_feriel@hotmail.com (F. Bouatay), Sonia.dridi@hotmail.com (S. Dridi-Dhaouadi), drira.neila@hotmail.com (N. Drira), farouk.mheni@gmail.com (M. Farouk Mhenni)

Received 4 February 2015; Accepted 3 June 2015

ABSTRACT

The valorization of a low-cost and an abundant material is a significant work for environmental protection. The objective of this work was to investigate the adsorption of two dyes: Basic Red 46 (BR46) and Reactive Yellow 181 (RY181) onto raw (S1) and modified clays. These modifications were carried out by calcination at different temperature (S2, S3, ..., S9), acidic activation, and acetylation. The surface properties of the adsorbents were characterized by the cation exchange capacity, Fourier transform infrared, and X-ray diffraction analyses. Batch studies were performed to evaluate the effect of the contact time and initial dye concentrations on the removal capacities of adsorbents. Among the kinetic models tested, the adsorption kinetics was best described by the pseudo-second-order equation. The isotherm data fitted well with Langmuir model. The maximum adsorption capacities onto the raw clay (S1), calcined clay at 600˚C (S5), acidic activated clay (AC), and acetylated clay (MC) were 2.805, 4.232, 1.968, and 2.756 mmol/g for CI Basic Red 46 and 0.031, 0.030, 0.046, and 0.050 mmol/g for CI Reactive Yellow 181, respectively.

Keywords: Adsorption; Anionic dye; Cationic dye; Modified clay

1. Introduction

Nowadays, with the rapid development of textile activities such as dyeing, printing, coating, and leather industries, the environmental contamination associated with the chemical products in wastewater has drawn much attention. It is estimated that more than 70.000 tones of synthetic dyes are discharged in effluent from textile industry in the world every year [1]. The dyes released during textile clothing, printing, and dyeing process are considered as hazardous and toxic to some organisms and may cause harmful effects to aquatic creatures [2]. In fact, the synthetic dyes usually contain azo-aromatic groups which are of extreme environmental concern due to their carcinogenic, mutagenic, and inert properties. This complex aromatic structure involved physicochemical, thermal, and optical stability which made it resistant to conventional wastewater treatment [3].

Therefore, several researches were carried out using different treatment technologies for pollutant removal from wastewater, such as chemical coagulation–floculation process [4,5], oxidation process [6,7], biological treatment [8,9], membrane-based separation processes [10,11] and adsorption [2,12,13].

*Corresponding author.

Furthermore, the adsorption process is the most efficient method of removing pollutants from wastewater. It presents several advantages such as simplicity and low-cost operation (compared to separation processes) without sludge formation [14]. In this regard, the most commonly used adsorbent for wastewater treatment was the activated carbon due to its large specific surface area and its high adsorption capacity. Despite the effectiveness, this adsorbent is expensive and difficult to regenerate after use. So, there is a need to look for relatively cheap adsorbents that can be applied for water pollution control. Therefore, studies indicated that many materials such as sewage sludge [15], cellulose [16], agriculture residues [17,18], and natural clay [19–21] were used as effective adsorbents for dyes removal.

In this regard, many researches in recent years have focused on the use of bio-adsorbents for pollutant retention due to their high specific surface area. Among these alternative adsorbents, bentonite [22], montmorillonite [23], alunite [24], sepiolite [25], zeolite [26], kaolinite [3], diatomite [27], and hydrocalcite [28] can be cited.

In order to increase their adsorption capacities, modified clays have been identified as an innovative and promising class of adsorbent materials. The adsorption behavior of the anionic dyes onto polydiallydimethylammonium-modified bentonite (PDADMA bentonite) was studied in single, binary, and ternary dye system [14]. Bouberkaa et al. used different clays (exchanged with sodium and hydroxyaluminic polycation pillared clays) for the anionic dye Supranol Yellow 4GL removal. This study showed that the modified clay has a high adsorption capacity for some textile dyes [29].

Furthermore, cationic dyes are the cheapest and the brightest synthetic chemicals among the commercial dye range. Besides, reactive dyes are also considered as an important class of textile dyes due to their good fastness properties and higher brightness. These contain chromophore groups such as azo, anthraquinone, triarylmethane, phthalocyanine, formazan, and oxazine which lead to a covalent bond with the fiber [30]. In the other hand, the high solubility in water of these basic and reactive dyes makes difficult their removal using conventional chemical treatment. So, adsorption process appears to be the best prospect for the elimination of these dyes. In this regard, several researches were investigated concerning the ability of modified clay to adsorb reactive and basic dyes [31,32].

The purpose of this study was to test the possibility of using locally available clay for cationic and anionic dyes adsorption. Basic Red 46 (BR 46) and Reactive Yellow 181 (RY181) were selected as synthetic azo dye models due to their extensive use in textile industry. Thermally treated and surface modified clays (acidic and acetyl activations) were used to improve the adsorption capacity of the raw clay. Surface characterization, kinetic, and equilibrium experiments were performed to study the adsorption behavior of these materials.

The relevance of this work is to use both the macroscopic and microscopic data to understand the adsorption mechanism and to evaluate the dye removal.

2. Experimental

2.1. Adsorbate

The dyestuffs used as adsorbates in this study are C.I. Basic Red 46 (BR46) ($C_{19}H_{26}N_6O_4S$) and the C.I Reactive Yellow 181 (RY181) ($C_{24}H_{24}Cl–N_9O_{12}S_3Na_3$), supplied by Ciba Company. Their molecular mass are respectively M_r = 432.00 g/mol and M_r = 830.45 g/mol, and their molecular structures are shown in Fig. 1. The UV–vis spectra of the dyestuffs aqueous fraction were recorded using a CECIL 2021 Instruments UV–vis spectrophotometer, and the results are represented in Fig. 2. The maximum wavelengths λ_{max} of these dyes were found to be 530 and 413 nm, respectively.

2.2. Adsorbent preparation

Clays used in this research were collected from eastern Tunisia in the region of Monastir. The preparation processes of the studied adsorbents are presented in Fig. 3. All other chemicals used in this study were obtained from Sigma Aldrich, France. The sieving of samples were performed using ASTM standard sieves.

2.3. Adsorbent characterization

The cation exchange capacity (CEC) of the studied sample was obtained by adding about 0.2 g of adsorbent (dried at 110˚C) to 25 ml of 0.5 M $CaCl_2{\cdot}2H_2O$ solution. The flask was shaken for 1 h and allowed to settle overnight. The residue was filtered and washed with methanol (75%) for 4–5 times and then with distilled water to free it from chloride. Thirty milliliter of KCl 1 M was added to the residue left in filter paper for slow leaching. Finally, the filtrate was titrated with EDTA 0.01 M. The value of CEC was calculated from the amount of Ca^{2+} released [33].

Fourier transform infrared (FTIR) spectra were recorded on a Perkin–Elmer IR-197 spectrophotometer using potassium bromide disks. A total of 32 scans for

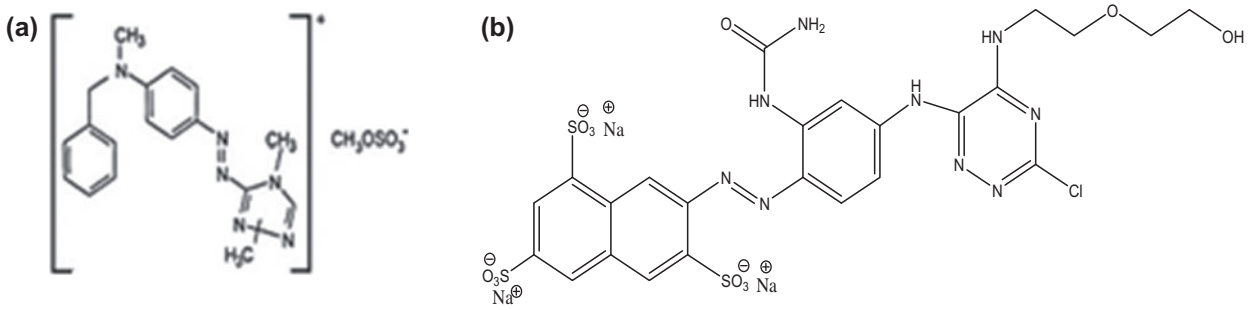

Fig. 1. Molecular structure of dyestuffs: (a) Basic Red 46 and (b) Reactive Yellow 181.

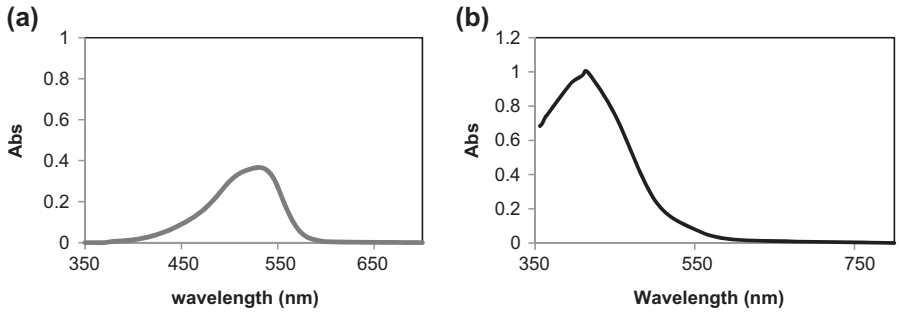

Fig. 2. UV–vis spectra of dyestuffs: (a) Basic Red 46 and (b) Reactive Yellow 181.

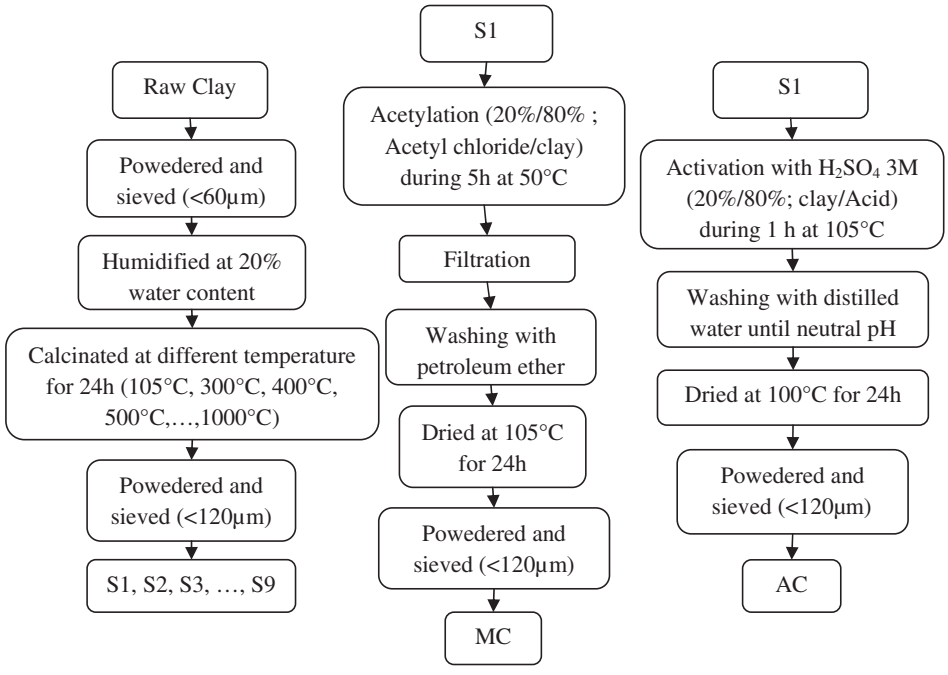

Fig. 3. The preparation processes of studied adsorbents.

each sample were taken with a resolution of 4 cm^{-1}, with a range of 4,000–400 cm^{-1}

The X-ray diffraction analysis was carried out using a Philips X´ Pert Pro system. The X-ray generator was operated at 40 kV and 40 mA, and Cu-Kα radiation was used.

2.4. Adsorption study

2.4.1. Kinetic study

Adsorption kinetic experiments were carried out mixing 25 ml of a constant dye solution concentration (100 mg/L) with 0.075 g of adsorbent at 20°C, pH 6, and a constant stirring speed of 150 rpm. Samples were centrifuged at 2,000 rpm for 10 min, and the supernatant absorbance was measured using colorimetric method.

Several kinetic models are available to examine the controlling mechanism of the adsorption process and to fit the experimental data [19]. Four common kinetic models were tested: pseudo-first-order, pseudo-second-order, the Elovich, and the intraparticle diffusion models. The kinetic models equations are presented in Table 1.

2.4.2. Isotherm study

Adsorption isotherm experiments were carried out mixing 25 ml of an aqueous dye solution with different dye concentrations with 0.075 g of adsorbent at

Table 1
The kinetic model equations

Model	Equation	References
Pseudo-first order model	$q_t = q_e[1 - \exp(-K_1 t)]$ (1) where q_e and q_t are the amounts of dye adsorbed per unit of adsorbent (mmol/g) at equilibrium time and time t, respectively, and K_1 (1/min) is the rate constant for the first-order kinetics	[36]
Pseudo-second order model	$q_t = \frac{K_2 q_e^2 t}{1 + q_e K_2 t}$ (2) where K_2 (g/mmol min) is the rate constant of adsorption, q_e is the amount of dye adsorbed at equilibrium (mmol/g), and q_t is the amount of dye adsorbed at time t (mmol/g)	[37]
Elovich model	$q_t = \frac{1}{\beta}\ln(\alpha\beta) + \frac{1}{\beta}\ln(t)$ (3) where α (mmol/g) is the initial adsorption rate constant and the parameter β (g/(mmol min)) is related to the extent of surface coverage and activation energy for chemi-adsorptions	[38]
Intraparticle diffusion model	$q_t = K_p t^{1/2} + C$ (4) where K_p represents intraparticle diffusion rate constant (mmol/g/$min^{1/2}$), and C is a constant (mmol/g) which gives information about the thickness of boundary layer	[39]

Table 2
The isotherm model equations

Model	Equation	References
Langmuir model	$\frac{C_e}{q_e} = \frac{1}{Q_m K_L} + \frac{1}{Q_m} C_e$ (5) where q_e (mmol/g) is the amount of adsorbate per unit mass of adsorbent, C_e (mmol/L) is the equilibrium concentration of the adsorbate, and Q_m (mmol/g) and K_L(L/mmol) are Langmuir constants related to adsorption capacity and rate of adsorption, respectively	[40]
Freundlich model	$q_e = K_F C_e^{1/n}$ (6) where K_F ((mmol$^{n-1/n}$ $L^{1/n}$)/g) is roughly an indicator of the adsorption capacity and $1/n$ is the adsorption intensity	[41]
Temkin model	$q_e = B \ln A + B \ln C_e$ (7) where $B = \frac{RT}{b}$, T is the absolute temperature in K, R is the universal gas constant, A (mmol/L) is the equilibrium binding constant, and B (L/g) is related to the heat of adsorption	[42]

20°C, pH 6, and a constant stirring speed of 150 rpm for 24 h. Samples were centrifuged at 2,000 rpm for 5 min, and the supernatant absorbance was measured using colorimetric method.

In order to establish the most appropriate equilibrium data correlations for the adsorption system, three common isotherm models were tested: Langmuir, Freundlich, and Temkin models. The isotherm models' equations are presented in Table 2.

2.5. Recycling and regeneration process of studied adsorbent

In this research, the recovery study of the raw and calcinated clays was carried out after the adsorption of real effluent pollutants. The wastewater was taken from a Tunisian dyeing and finishing of Denim Fabrics industry, and its characteristics are presented in Table 3. The already used was recovered by calcinations at 600°C for one hour and re-tested for the decolorization and COD removal of the textile effluent for five times.

The absorbance of the effluent was recorded using a CECIL 2021 Instrument UV–vis spectrophotometer. The color removal (decolorization (%)) and the chemical oxygen demand (COD) removal were calculated according to Eqs. (8) and (9), respectively.

$$\text{decolorization}\,(\%) = \frac{\text{Abs}_i - \text{Abs}_f}{\text{Abs}_i} \times 100 \quad (8)$$

where Abs_i and Abs_f are the absorbance (measured at the maximum wavelength) of the dye bath solution and the supernatant after adsorption treatment, respectively.

$$\text{COD removal}\,(\%) = \frac{\text{COD}_i - \text{COD}_f}{\text{COD}_i} \times 100 \quad (9)$$

where $\text{COD}_i\,(\text{mgO}_2/\text{L})$ and $\text{COD}_f\,(\text{mgO}_2/\text{L})$ are the chemical oxygen demands of the effluent before and after adsorption treatment, respectively.

Table 3
Studied effluent characteristics

pH	11.9
Maximum wavelength λ_{max} (nm)	630
Abs	10.67
COD (mg O_2/l)	2,350
Conductivity (mS/cm)	3.6
Turbidity (NTU)	38

3. Results and discussions

3.1. Adsorbents characterizations

3.1.1. Surface characterization

The cation exchange capacities (CEC) of the studied clay materials are presented in Table 4.

For the modified clay samples, chemical and thermal treatment had no effect on the CEC of the studied adsorbents. In fact, the CEC values varied from 14.8 meq/g for the calcinated clay at 1,000°C (S9) to 15.8 meq/g for the calcinated clay at 600°C (S5) and from 14.6 meq/g for the acidic activated samples (AC) to 15.1 meq/g for the acetylated modified adsorbents (MC).

3.1.2. Fourier transform infrared (FTIR) analysis

The FTIR spectroscopy analysis of the calcinated clays (S5 and S9) is shown in Fig. 4(a), and the FTIR analysis of the chemically modified adsorbents is represented in Fig. 4(b). The FTIR spectrum of the raw clay (dried at 105°C) was used as a reference for interpreting any possible structural changes after modifications.

The raw clay spectrum presents a vibration band at 3,620 cm^{-1} characteristic of (Al–O–Al) and deformation at 915 cm^{-1} which indicate that the raw clay is dioctahedral. The deformation band at 1,630 cm^{-1} is characteristic of the water hydroxyl vibrations in the raw clay. The strong bands at 1,100–1,000 cm^{-1} are characteristic of stretching vibrations of (Si–O) in the plane and out of plane.

Furthermore, the vibration bands of (Al–O–Al) at 3,620 and 915 cm^{-1} disappeared after chemical and thermal modifications. Besides, the water hydroxyl vibrations disappeared for the calcinated materials (S5 and S9). So, it shows that after modification, clay materials change their structure and there is a thermal decomposition of alunite. In fact, this decomposition occurs in two main stages. The first stage is the loss of water vapor; the decomposition pressure reaching one atmosphere at 500°C. The second stage was the formation of γ–Al_2O_3 during calcination up to 600°C. Moreover, there is a decrease of the Si–O vibration band at

Table 4
Calcination temperature and the CEC values for the studied adsorbents

Samples	S1	S5	S9	MC	AC
Calcination temperature (°C)	100	600	1,000	–	–
CEC (meq/g)	15.4	15.8	14.8	15.1	14.6

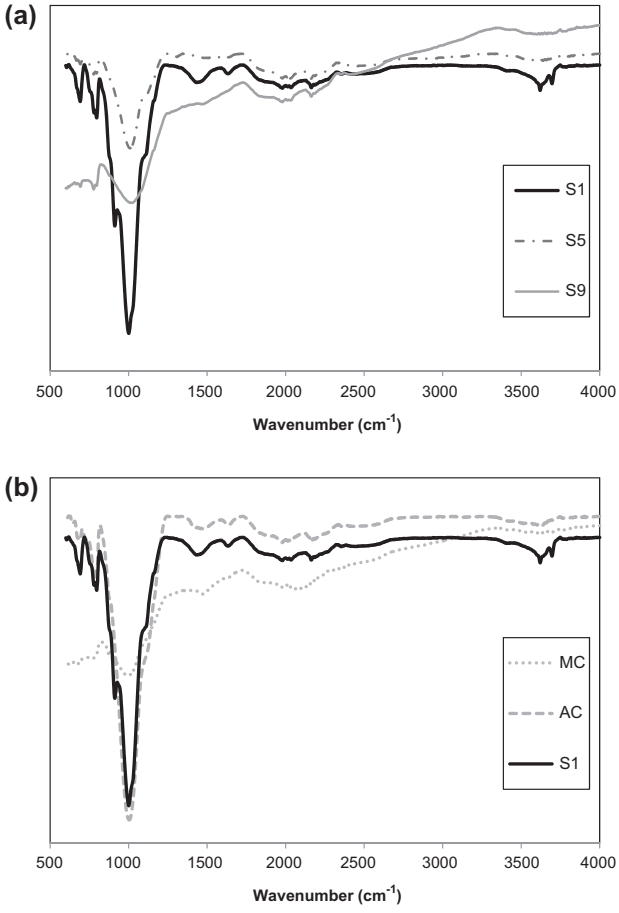

Fig. 4. The FTIR spectra of the studied adsorbents: (a) calcinated clays and (b) chemically modified clay.

1,100 cm^{-1} and the stretching vibrations between 650 and 950 cm^{-1} containing the area of absorbing vibration characteristics of phyllosilicates at 910 cm^{-1} and Al–O at 720–780 cm^{-1} for the modified adsorbents.

3.1.3. The X-ray diffraction analysis

In the X-ray diffraction pattern of the studied clay materials (Fig. 5), the main reflections of S1 were also present in the modified adsorbents but with a slight change in intensity and flex width. This implied that only significant amount of clay particles had undergone modification treatment. The two peaks at 7.14 and 3.33 Å are the characteristic peaks of kaolinite clay mineral [34]. For the thermally and chemically modified clay samples, we noticed the disappearance of the characteristic peak of kaolinite at 7.14 Å due to the high temperature (thermal modification) and the grafting of anionic sites (chemical modification) used during the modification treatment.

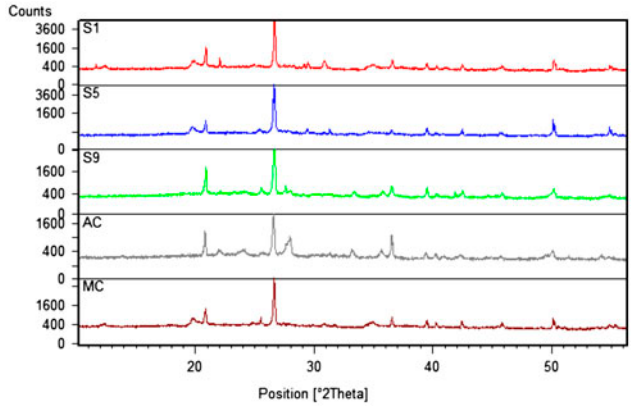

Fig. 5. The X-ray diffraction analysis patterns of the studied clay materials.

So, FTIR and X-ray diffraction analyses of the different studied adsorbents showed that the thermal modification probably changed the structure of the clay materials in terms of porous volume and adsorption sites [24]. These modifications could have an effect on the dye adsorption capacity. The adsorption behavior of these modified clay materials were studied in the following sections.

3.2. Adsorbent study

3.2.1. Effect of calcination temperature

The raw clay was calcinated at temperature ranging from 300°C to 1,000°C for 24 h. The adsorption experiments with these clays (S2 to S9) using aqueous solution of BR 46 and RY 181 with a dye concentration of 100 mg/L were performed. The results are shown in Fig. 6.

It can be seen from Fig. 6 that the dye adsorption was enhanced by calcination. Hence, the dye adsorption capacity increases with the increase of calcination

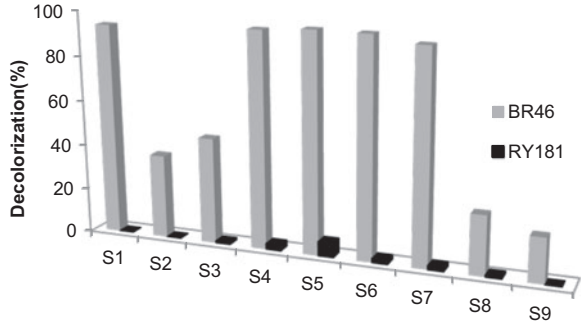

Fig. 6. The dye removal of Basic Red 46 and Reactive Yellow 181 onto calcinated clays.

temperature (from 300 to 600˚C). However, above a temperature of 600˚C, the adsorption capacity started to decrease. This can be related to the thermal decomposition of alunite which was observed on the FTIR analysis. Indeed, at 600˚C, the alunite structure changes from γ–Al_2O_3 (orthorhombic) to α–Al_2O_3 (Hexagonal) [24].

The kinetic, isotherm, and pH studies were carried out on the samples S5 and S9 calcinated at 600 and 1,000˚C, respectively, and on the chemically modified clays MC and AC and compared with the raw clay S1.

3.2.2. Kinetic study

The experimental kinetic curves are presented in Fig. 7. The parameters calculated for the different models are given in Tables 5 and 6.

From the kinetic curves, it is obvious that the amount of the adsorbed dyes onto clay materials increases with time until a constant value beyond which no more dye removal from aqueous solution was observed. The contact time necessary for basic dye to reach saturation was about 10 min, while 120 min was necessary for reactive dye.

Moreover, it is obvious that for the same initial mass of the adsorbent and dye concentration, the retention rate was most important for basic dye adsorption. In fact, at the equilibrium, the adsorption capacities of the studied clay materials varied from 0.0292 to 0.068 mmol/g for the BR 46 and from 0.0021 to 0.0056 mmol/g for the RY181.

In this regard, the adsorption capacities, at equilibrium, for the raw clay (S1), the thermally modified clays (S5 and S9), the acidic activated clay (AC), and the acetylated modified clay (MC) were 0.0675, 0.0687,

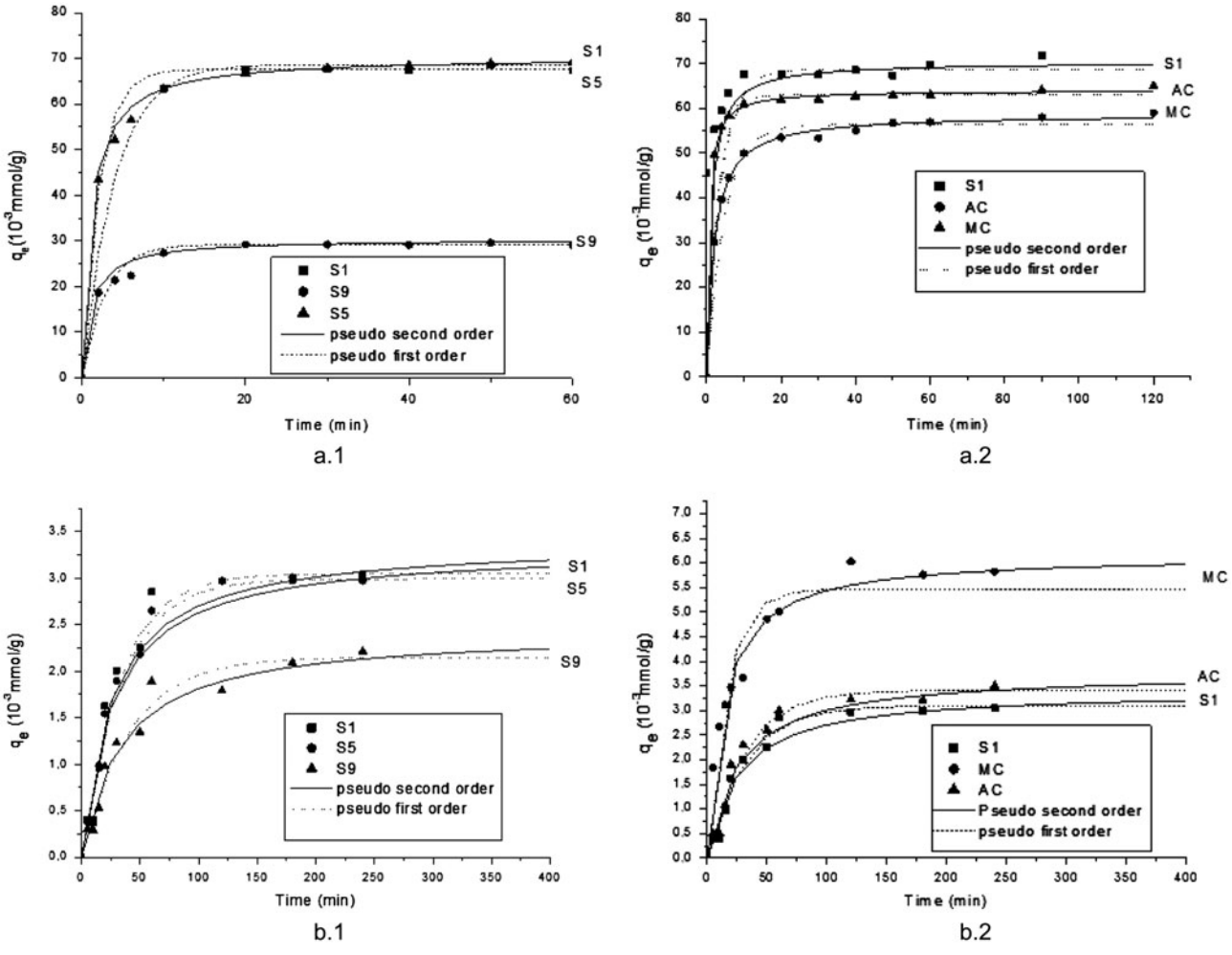

Fig. 7. The kinetic curves of BR 46 and RY 181 retention by adsorbent materials: (a.1) calcinated clay onto BR46; (a.2) activated and chemically modified clay onto BR46; (b.1) calcinated clay onto RY181; and (b.2) activated and chemically modified clay onto RY181.

Table 5
The kinetic parameters of Basic Red 46 adsorption

	Pseudo-first-order			Pseudo-second-order			Intraparticle diffusion		
	q_e (mmol/g)	K_1 (1/min)	R^2	q_e (mmol/g)	K_2 (g/mmol min)	R^2	K_p (mmol/g/min$^{1/2}$)	C (mmol/g)	R^2
S1	0.0675	0.499	0.988	0.0701	0.013	0.998	4.152	37.71	0.49
S5	0.0687	0.254	0.996	0.0704	0.012	0.997	5.161	29.06	0.56
S9	0.0292	0.360	0.961	0.0306	0.213	0.984	1.948	14.95	0.56
MC	0.0616	0.752	0.993	0.0636	0.028	0.999	3.331	38.72	0.393
AC	0.0544	0.334	0.986	0.0582	0.009	0.999	3.939	26.533	0.618

Table 6
The kinetic parameters of Reactive Yellow 181 adsorption

	Pseudo-first-order			Pseudo-second-order			Intraparticle diffusion		
	q_e (mmol/g)	K_1 (1/min)	R^2	q_e (mmol/g)	K_2 (g/mmol min)	R^2	K_p (mmol/g min$^{1/2}$)	C (mmol/g)	R^2
S1	0.0030	0.0313	0.944	0.0033	0.0014	0.974	0.076	1.163	0.44
S5	0.0029	0.0298	0.959	0.0033	0.112	0.977	0.074	1.127	0.433
S9	0.0021	0.0245	0.956	0.00243	0.0119	0.969	0.059	0.687	0.544
MC	0.0055	0.0496	0.953	0.00647	0.00926	0.983	0.146	2.713	0.56
AC	0.0033	0.0322	0.955	0.00375	0.0105	0.975	0.081	1.303	0.464

0.0292, 0.0544, and 0.06162 mmol/g for BR46 and 0.003, 0.0029, 0.0021, 0.0033, and 0.0056 mmol/g for RY181, respectively. Clearly, the adsorption behavior and capacities varied depending on the nature of dye and the modification treatment on the clay materials.

Moreover, the kinetic data obtained gave bad fit with intraparticle diffusion model. However, a good fit was obtained with the pseudo-first-order and pseudo-second-order models as shown by the high correlation coefficients evaluated in these cases (R varied from 0.961 to 0.999).

The adsorption of both cationic and anionic dyes onto the studied clay materials was through chemisorption and physisorption. In fact, dyes are adsorbed mainly through hydrophobic and electrostatic attractions, hydrogen bonding, surface function group, and cation exchange between the clay materials and the dyes. In this regard, the high affinity of the basic dye onto the clay materials could be due to the chemical attraction between the negatively charged surface of the clay and the approaching colored dye cations. But, the lower affinity of the anionic dye could be attributed to the repulsive force between anionic groups of reactive dye and the negatively charged surface of the clay adsorbents.

On the other hand, the number of hydrophobic sites decreases for clay calcinated at temperature higher than 600˚C, and thus, the adsorption capacity of these basic and reactive dyes onto the thermally modified samples decreased. Hence, the chemical modification increases the electrostatic interactions between the clay samples and cationic dye and improves their affinity for reactive dyes.

3.2.3. Isotherm study

The isotherm curves of the different studied adsorbents and dyes are represented in Fig. 8. The modelization study was made to fit isotherm experimental data with Langmuir, Freundlich, and Temkin models. The different model parameters are presented in Tables 7 and 8 and showed that the isotherm data gave the best fit with Langmuir model since the correlation coefficient R varied between 0.97 and 0.99.

The maximum adsorbed amount, Q_m (mmol/g), evaluated from Langmuir model, indicated that the calcinated clay at 600˚C (S5) had the highest adsorption capacity for the basic dye (4.243 mmol/g), and this amount decreases after calcination at 1,000˚C. This result supports the previous conclusion: A high calcination temperature changes the clay materials structure, and hence, the hydrophobic interactions decrease after thermal degradation. Moreover, the amount of the adsorbed basic dye decreases after chemical activations.

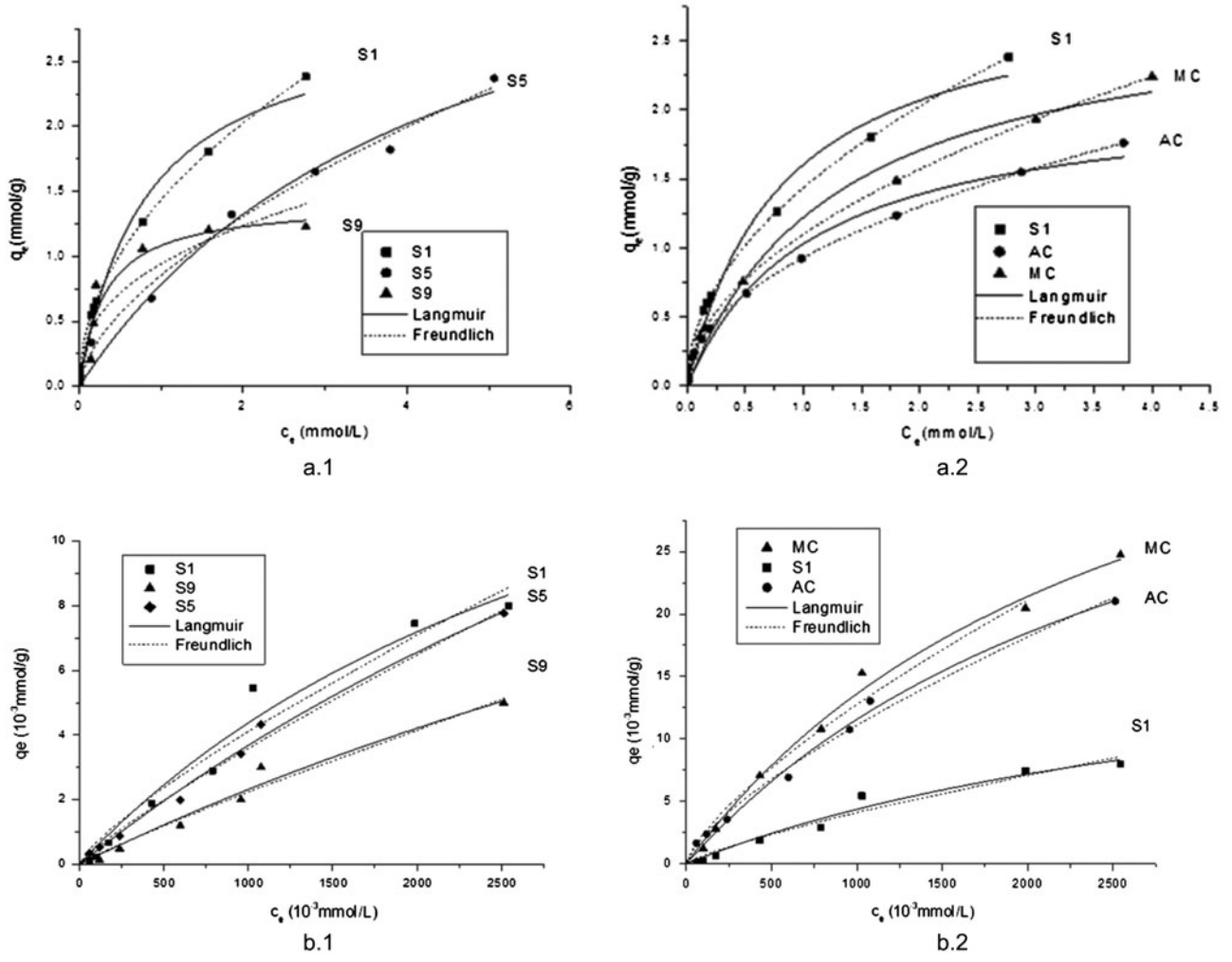

Fig. 8. The isotherm curves of BR 46 and RY 181 retention by adsorbent materials: (a.1) calcinated clay onto BR46; (a.2) activated and chemically modified clay onto BR46; (b.1) calcinated clay onto RY181; and (b.2) activated and chemically modified clay onto RY181.

Table 7
The isotherm parameters of Basic Red 46 adsorption

	Langmuir			Freundlich			Temkin		
	Q_m (mmol/g)	K_L (L/mmol)	R^2	K_F (mmol$^{n-1/n}$ L$^{1/n}$/g)	n	R^2	A (mmol/L)	B (g/(mmol min))	R^2
S1	2.805	1.225	0.978	46.49	2.01	0.974	1.287	267.67	0.84
S5	4.2432	0.226	0.988	12.604	1.637	0.994	0.842	193.63	0.788
S9	2.4529	0.022	0.994	3.383	1.425	0.989	0.0227	214.85	0.841
MC	2.756	0.76142	0.996	31.93	1.95	0.994	0.234	248.93	0.849
AC	1.968	0.9363	0.986	2.07	2.07	0.980	0.127	217.41	0.837

Besides, the maximum adsorption capacities of the modified clay materials increase for the reactive dye since the acetylated clay exhibited the highest adsorption capacity (0.050 mmol/g). The improvement of the reactive dye affinity could be due to the grafting of new cationic sites on the clay surface after chemical modification.

Tables 7 and 8 showed that the highest retention capacities were obtained for the basic dye regardless of the adsorbent. This result could be explained by the

Table 8
The isotherm parameters of Reactive Yellow 181 adsorption

	Langmuir			Freundlich			Temkin		
	Q_m (mmol/g)	K_L (L/mmol)	R^2	K_F (mmol$^{n-1/n}$ L$^{1/n}$/g)	n	R^2	A (mmol/L)	B (g/(mmol min))	R^2
S1	0.031	0.00016	0.970	0.0091	1.12	0.965	0.0106	2.0102	0.856
S5	0.030	0.00014	0.993	0.00981	1.17	0.991	0.0105	1.820	0.828
S9	0.023	0.00011	0.979	0.0044	1.11	0.976	0.0091	1.239	0.827
MC	0.050	0.00038	0.993	0.0844	1.38	0.985	0.011	6.376	0.932
AC	0.0460	0.00034	0.993	0.0823	1.40	0.992	0.0137	4.896	0.863

hydrophobic and electrostatic attractions in addition to the high CEC of the studied materials.

3.3. Sorption mechanism study

The surface characterization of raw clay and thermally and chemically modified clays showed that the different modifications changed the structure of the clay materials in terms of porous, volume, and adsorption sites.

The kinetic and isotherm studies showed that these modifications have an effect on the adsorption dye capacities and the adsorption mechanism. In fact, the macroscopic study showed that the adsorption of both cationic and anionic dyes onto studied clay materials was though chemisorptions and physisorption. Hence, the studied dyes were adsorbed through hydrophobic and electrostatic attractions, hydrogen bonding, surface function groups, and cation exchange.

3.4. Recycling and regeneration process of used materials

Porous materials that are thermally stable are actually in great demand. So, recycling and regeneration of the used adsorbent is considered as an important economical aspect to minimize the cost of the process. The literature showed that the recovery of clay materials through thermal treatment was achieved at high temperature (550˚C) and time (30 min). Beyond these conditions, the recovery of the already used adsorbents began to decrease [3].

The results of the regeneration study done in the same conditions are presented in Fig. 9. From this figure, it is obvious that the removal efficiency improved as the number of recovery cycles increased. In fact, the heat generated during calcination decomposed the organic adsorbates to carbon, which is then oxidized to carbon oxides in air, leaving the bared surface available for re-adsorption.

Meanwhile, heat treatment at a very high temperature can also break down the bond structure of the material and cause the collapsing of the pores. In this conditions, the specific surface area and pore volume could be reduced and result in lower adsorption capacity of the adsorbent [35].

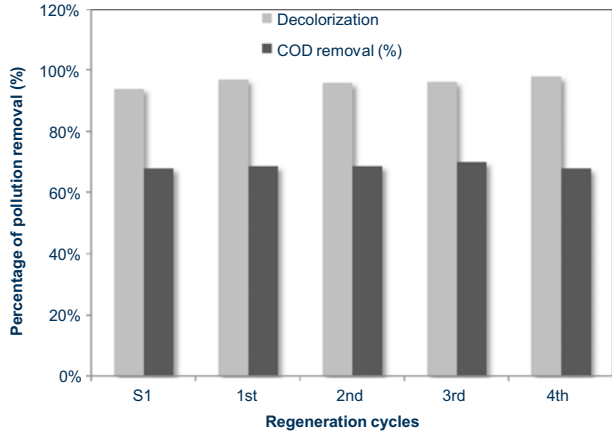

Fig. 9. Recovery and life span of the raw clay after calcination at 600˚C during 30 min.

4. Conclusion

The adsorption of both cationic and anionic dyes onto the studied clay materials was achieved through chemisorption and physisorption. But, high adsorption capacities were observed for basic dye onto clay. In fact, the studied dyestuffs are adsorbed mainly through hydrophobic and electrostatic attractions, hydrogen bonding, surface function group, and cation exchange between the clay materials and the dyes. In this regard, the high affinity of the basic dye onto the clay materials could be due to the chemical attraction between the negatively charged surface of the clay and the approaching colored dye cations. But, the anionic dyes are not adsorbed by electrostatic attractions, and hydrophobic attraction (HA) is probably the most predominant mechanism.

On the other hand, the acetylation of the raw clay increased the adsorption affinity of the surface for the reactive dye due to the increased electrostatic attraction between the charged grafting groups on the clay surface and the anionic dye. But, for the calcinated clay at temperature higher than 600˚C, the number of hydrophobic sites decreases; therefore, the adsorption capacity of these basic and reactive dyes onto the thermally modified samples decreased.

Acknowledgments

The authors are particularly grateful to Mr Mohamed Touzi, the G.D of SITEX (Société Industrielle des Textiles); Mr Moez Kechida, the development engineer in SITEX; and all the technical and administrative staff of this company for their assistance and valuable contribution. This research and innovation paper was performed in the framework of a MOBIDOC thesis funded by the European Union under the program PASRI.

References

[1] W. Zhang, H. Li, X. Kan, L. Dong, H. Yan, Z. Jiang, H. Yang, Adsorption of anionic dyes from aqeous solutions using chemically modified straw, Bioresour. Technol. 117 (2012) 40–47.
[2] E. Errais, J. Duplay, M. Elhabiri, M. Khodja, R. Ocampo, R. Baltenweck-Guyot, F. Darragi, Anionic RR120 dye adsorption onto raw clay: Surface properties and adsorption mechanism, Colloids Surf., A Physicochem. Eng. Asp. 403 (2012) 69–78.
[3] V. Vimonses, Shaomin Lei, B. Jin, Chris W.K. Chow, C. Saint, Adsorption of congo red by three Australian kaolins, Appl. Clay Sci. 43 (2009) 465–472.
[4] T.H. Kim, C. Park, J. Yang, S. Kim, Comparison of disperse and reactive dye removals by chemical coagulation and Fenton oxidation, J. Hazard. Mater. 112 (2004) 95–103.
[5] Y. Zhou, Z. Liang, Y. Wang, Decolorization and COD removal of secondary yeast wastewater effluents by coagulation using aluminum sulfate, Desalination 225 (2008) 301–311.
[6] H.Y. Shu, W.P. Hsieh, Treatment of dye manufacturing plant effluent using an annular UV/H_2O_2 reactor with multi-UV lamps, Sep. Purif. Technol. 51 (2006) 379–386.
[7] F. Renault, B. Sancey, P.M. Badot, G. Crini, Chitosan for coagulation/flocculation processes—An ecofriendly approach, Eur. Polym. J. 45 (2009) 1337–1348.
[8] X. Lu, B. Yang, J. Chen, R. Sun, Treatment of wastewater containing azo dye reactive brilliant red X-3B using sequential ozonation and upflow biological aerated filter process, J. Hazard. Mater. 161 (2009) 241–245.
[9] H. Wang,X.W. Zheng, J. Su, Y. Tian, X.J. Xiong, T.L. Zheng, Biological decolorization of the reactive dyes Reactive Black 5 by a novel isolated bacterial strain *Enterobacter* sp. EC3, J. Hazard. Mater. 171 (2009) 654–659.
[10] J. Hwan Mo, Y. Lee, J. Kim, J.M. Jeong, J. Jegal, Treatment of dye aqueous solutions using nanofiltration polyamide composite membranes for the dye wastewater reuse, Dyes Pig. 76 (2008) 429–434.
[11] W.L. Lau, A.F. Ismail, Polymeric nanofiltration membranes for textile dye wastewater treatment: Preparation, performance evaluation, transport modelling, and fouling control—A review, Desalination 245 (2009) 321–348.
[12] C.H. Weng, Y.F. Pan, Adsorption of a cationic dye (methylene blue) onto spent activated clay, J. Hazard. Mater. 144 (2007) 355–362.
[13] L.C.A. Oliveira, M. Gonçalves, D.Q.L. Oliveira, M.C. Guerreiro, L.R.G. Guilherme, R.M. Dallago, Solid waste from leather industry as adsorbent of organic dyes in aqueous-medium, J. Hazard. Mater. 141 (2007) 344–347.
[14] D. Shen, J. Fan, W. Zhou, B. Gao, Q. Yue, Q. Kang, Adsorption kinetics and isotherm of anionic dyes onto organo-bentonite from single and multisolute systems, J. Hazard. Mater. 172 (2009) 99–107.
[15] H. Dhaouadi, F. M'Henni, Vat dye sorption onto crude dehydrated sewage sludge, J. Hazard. Mater. 164 (2009) 448–458.
[16] N. Ben Douissa, L. Bergaoui, S. Mansouri, R. Khiari, M.F. Mhenni, Macroscopic and microscopic studies of methylene blue adsorption onto extracted celluloses from *Posidonia oceanic*, Ind. Crops Prod. 45 (2013) 106–113.
[17] E.C. Lima, B. Royer, J.C.P. Vaghetti, N.M. Simon, B.M. da Cunha, F.A. Pavan, E.V. Benvenutti, R. Cataluña-Veses, C. Airoldi, Application of Brazilian pine-fruit shell as a biosorbent to removal of reactive red 194 textile dye from aqueous solution, J. Hazard. Mater. 155 (2008) 536–550.
[18] F.A. Pavan, E.C. Lima, S.L.P. Dias, A.C. Mazzocato, Methylene blue biosorption from aqueous solutions by yellow passion fruit waste, J. Hazard. Mater. 150 (2008) 703–712.
[19] E. Errais, J. Duplay, F. Darragi, I. M'Rabet, A. Aubert, F. Huber, G. Morvan, Efficient anionic dye adsorption on natural untreated clay: Kinetic study and thermodynamic parameters, Desalination 275 (2011) 74–81.
[20] M.S. Rehman, M. Munir, M. Ashfaq, N. Rashid, M.F. Nazar, M. Danish, J. Han, Adsorption of Brilliant Green dye from aqueous solution onto red clay, Chem. Eng. J. 228 (2013) 54–62.
[21] T.B. Lyim, G. Güçlü, Removal of basic dyes from aqueous solutions using natural clay, Desalination 249 (2009) 1377–1379.
[22] Q.H. Hu, S.Z. Qiao, F. Haghseresht, M.A. Wilson, G.Q. Lu, Adsorption study for removal of basic red dye using bentonite, Ind. Eng. Chem. Res. 45 (2006) 733–738.
[23] A.H. Gemeay, Adsorption characteristics and the kinetics of the cation exchange of rhodamine-6G with Na+-montmorillonite, J. Colloid Interface Sci. 251 (2002) 235–241.
[24] M. Özacar, I.A. Sengil, Application of kinetic models to the sorption of disperse dyes onto alunite, Colloids Surf. 242 (2004) 105–113.
[25] M. Doğan, Y. Özdemir, M. Alkan, Adsorption kinetics and mechanism of cationic methyl violet and methylene blue dyes onto sepiolite, Dyes Pigm. 75 (2007) 701–713.

[26] S.K. Alpat, Ö. Özbayrak, Şenol Alpat, H. Akçay, The adsorption kinetics and removal of cationic dye, Toluidine Blue O, from aqueous solution with Turkish zeolite, J. Hazard. Mater. 151 (2008) 213–220.
[27] M.A.M. Khraisheh, M.A. Al-Ghouti, S.J. Allen, M.N. Ahmad, Effect of OH and silanol groups in the removal of dyes from aqueous solution using diatomite, Water Res. 39 (2005) 922–932.
[28] N.K. Lazaridis, T.D. Karapantsios, D. Georgantas, Kinetic analysis for the removal of a reactive dye from aqueous solution onto hydrotalcite by adsorption, Water Res. 37 (2003) 3023–3033.
[29] Z. Bouberka, S. Kacha, M. Kameche, S. Elmaleh, Z. Derriche, Sorption study of an acid dye from an aqueous solutions using modified clays, J. Hazard. Mater. 119 (2005) 117–124.
[30] V.K. Gupta, Application of low-cost adsorbents for dye removal – A review, J. Environ. Manage. 90 (2009) 2313–2342.
[31] S. Sonowane, P. Chaudhari, S. Ghodke, S. Phadtare, S. Meshran, Ultrasound assisted adsorption of basic dye onto organically modified bentonite, J. Sci. Ind. Res. 68 (2008) 162–167.
[32] F. Deniz, S. Karaman, Removal of Basic Red 46 dye from aqueous solution by pine tree leaves, Chem. Eng. J. 170 (2011) 67–74.
[33] S. Joong, J.A. Schwarz, Effect of HNO_3 treatment on the surface acidity of activated carbons, Department of Chemical Engineering and Materials Science, Syracuse University, Syracuse, NY, 1990, 13244.
[34] A. Hattab, M. Bagane, M. Chlendi, Characterization of tataouine's raw and activated clay, J. Chem. Eng. Process Technol. 155 (2013) 1–5.
[35] S. Wang, Z.H. Zhu, Characterisation and environmental application of an Australian natural zeolite for basic dye removal from aqueous solution, J. Hazard. Mater. 136 (2006) 946–952.
[36] S. Lagergren, About the theory of so-called adsorption of soluble substances, Kungliga Suenk, Vetenskapsakademiens, Handlinger Band. 24 (1889) 1–39.
[37] F. Bouatay, S. Dridi, M.F. Mhenni, Valorization of Tunisian pottery clay onto basic dyes adsorption, Inter. J. Environ. Res. 8 (2014) 1053–1066.
[38] S.J. Elovich, in: J.H. Schulman (Ed.), Proceedings of the Second International Congress on Surface Activity, 11, Academic Press, Inc, New York, NY, 1959, p. 253.
[39] D. Yue, Y. Jing, J. Ma, C. Xia, Removal of Neutral Red from aqueous solution by using modified hectorite, Desalination 267 (2011) 9–15.
[40] I. Langmuir, The adsorption of gases on plane surfaces of glass, mica and platinum, J. Am. Chem. 40 (1918) 1361–1403.
[41] H.M. Freundlich, Uber die adsorption in lösungen, Zeitschrift für Physikalische Chemie. 57 (1906) 385–470.
[42] M.J. Temkin, V. Pyzhev, Kinetics of ammonia synthesis on promoted iron catalysts, Acta Physiochim. URSS. 12 (1940) 217–222.